

# Free energy landscapes, dynamics and the edge of chaos in mean-field models of spin glasses

T. Aspelmeier,<sup>1</sup> R. A. Blythe,<sup>2,3</sup> A. J. Bray,<sup>2</sup> and M. A. Moore<sup>2</sup>

<sup>1</sup>*Institut für Theoretische Physik, Universität Göttingen,  
Friedrich-Hund-Platz 1, 37077 Göttingen, Germany*

<sup>2</sup>*School of Physics and Astronomy, University of Manchester, Manchester M13 9PL, U.K.*

<sup>3</sup>*School of Physics, University of Edinburgh, Mayfield Road, Edinburgh EH9 3JZ, U.K.*

(Dated: June 18, 2018)

Metastable states in Ising spin-glass models are investigated numerically by finding iterative solutions of mean-field equations for the local magnetizations  $m_i$ . A number of iterative schemes are employed, and two different mean-field equations are studied: the Thouless-Anderson-Palmer (TAP) equations that are exact for the Sherrington-Kirkpatrick model, and the simpler ‘naive-mean-field’ (NMF) equations, in which the Onsager reaction term of the TAP equations is omitted and which are exact for the Wallace model. The free-energy landscapes that emerge are very different for the two systems. For the TAP equations, the numerical studies confirm the analytical results of Aspelmeier et al., which predict that TAP states consist of close pairs of minima and index-one (one unstable direction) saddle points, while for the NMF equations the corresponding free-energy landscape contains saddle points with large numbers of unstable directions. For the TAP equations the free energy difference between a minimum and its adjacent saddle point (the ‘barrier height’) scales as  $1/(f - f_0)^{1/3}$  where  $f$  is the free energy per spin of the solution and  $f_0$  is the equilibrium free energy per spin. This means that for ‘pure states’ for which  $f - f_0$  is of order  $1/N$ , where  $N$  is the number of spins in the system, the barriers between them scale as  $N^{1/3}$ , but between states for which  $f - f_0$  is of order one, then the barriers are finite and also small so such metastable states will be of limited physical significance. For the NMF equations there are saddles of index  $K$  and we can demonstrate that their complexity  $\Sigma_K$  scales as a function of  $K/N$ .

We have also employed an iterative technique with a free parameter that can be adjusted to bring the system of equations close to the ‘edge of chaos’. Both for the TAP and NMF equations it is possible with this approach to find metastable states whose free energy per spin is close to  $f_0$ . As  $N$ , the number of spins is increased, it becomes harder and harder to find solutions near to the edge of chaos, but nevertheless the results which can be obtained are competitive with those achieved by more time-consuming computing methods and suggest that this method may be of general utility.

PACS numbers: 75.10.Nr, 75.50.Lk, 05.70.Ln

## I. INTRODUCTION

The study of metastable states in spin glasses began some 25 years ago with the calculations of Tanaka and Edwards [1] (TE) and of Bray and Moore [2] (BM), dealing with metastable states at zero and non-zero temperatures respectively, within the infinite-range Sherrington Kirkpatrick model. For the zero-temperature studies, metastable states were defined as states which are one-spin-flip stable, i.e. states for which flipping any one spin increases the energy, while for  $T > 0$  they were identified with solutions of the TAP equations [3], which are exact for the SK model. While the TE calculation is quite straightforward, the original BM calculation involved some technical challenges which were finessed in the first attempt, and have only recently been satisfactorily resolved, some 24 years after the original paper [4, 5, 6]. While the central result of BM, that the mean number (averaged over disorder configurations) of TAP solutions increases exponentially with the number of spins,  $\langle N_s \rangle \sim \exp[N\Sigma(T)]$ , where  $\Sigma(T)$  is the ‘complexity’, was confirmed by the later work, new insights into the nature of the TAP solutions and the structure

of the free-energy landscape were obtained. Specifically, it was found that all solutions correspond either to minima of the TAP free energy  $F_{\text{TAP}}$ , or to saddle points of index one, where the index of a saddle point is the number of negative eigenvalues of the Hessian matrix  $\partial^2 F_{\text{TAP}} / \partial m_i \partial m_j$ , so that minima have index zero. Furthermore, the minima and saddle points occur in close (in configuration space) pairs [5]. This structure has implications for the dynamics in the SK model. In particular we will study the free energy difference between the saddle and its associated nearby minimum. This difference would seem intuitively to be related to the barrier which has to be overcome to escape from a pure state and we will find that it increases with  $N$  like  $N^{1/3}$ . However, for the vast majority of the TAP states—all those with free energy per spin larger than its equilibrium value—the barriers are finite. This means that such TAP states are probably of little physical significance for the dynamics of the SK model.

We will contrast the TAP free-energy landscape with that of the naive mean-field (NMF) equations. We show numerically that the free-energy function  $F_{\text{NMF}}$  possesses saddle points with large indices  $K$  (up to a maximum proportional to  $N$ ), and we show that the correspond-

ing landscape is more rugged than the TAP landscape and tends to trap the ‘iterative’ dynamics at (or close to) a threshold free energy where the minima numerically dominate the saddle points, much as in the  $p$ -spin spherical model [7].

This qualitative distinction between dynamics on the TAP and NMF free energy surfaces is interesting because both sets of equations become *the same* at  $T = 0$ . In particular, they have the same ground states. This suggests a program for finding the ground-state energy by working with the TAP equations at very low but non-zero temperature, and using the resulting states at starting configurations for a final quench at  $T = 0$ . In view of the preceding discussion, the same approach applied to the NMF equations would not be successful, since the system would get stuck at a threshold free energy, as for the  $p$ -spin spherical model. If one hopes to determine ground-state properties using  $T > 0$  equations, therefore, it is important to choose equations with a favorable free-energy surface (like TAP) rather than an unfavorable one (like NMF). In other words if one is trying to find low energy states of (say) the SK model using standard algorithms such as gradient descent on a free energy surface, then one gets much lower energy solutions if one uses the exact free-energy surface than when one uses only an approximation to it. We suspect this point will have validity beyond the SK model.

However, we have discovered that it is possible to obtain solutions of low free energy by a method which takes one entirely off the free energy surface. These states are accessed through a novel iterative algorithm containing one adjustable parameter. We show that there is a critical value of this parameter separating runs which terminate from those which do not, and that the lowest free-energy states are accessed when the parameter is close to the critical value. As the parameter is increased towards the critical value, one sees many solutions which are limit cycles of a length which also increases as the critical value is approached and beyond the critical value only ‘chaotic solutions’ seem to exist. In the course of the iteration it is possible for the magnetizations to take unphysical values such that  $|m_i| > 1$ . We speculate that this approach may be a generic technique for finding low-cost states in hard optimization problems. Somehow being close to the ‘edge of chaos’ enables one to explore phase space and it is only the lowest states, which are surrounded by the highest barriers, which can trap the algorithm into a fixed point rather than a limit cycle. Possibly related ideas are in a paper by Boettcher and Frank [8].

The outline of the paper is as follows. In section II we state the TAP and NMF equations, discuss the algorithmic methods we will adopt and demonstrate that for NMF most of the standard algorithms seem to terminate at a free energy which is relatively insensitive to the algorithm. In section III, we explain this result by carrying out an exhaustive search for turning points of the free energy for small systems, showing that there is a threshold free energy below which minima numerically dominate

saddle points. The connection between the structure of the free-energy landscape and the nature of the dynamical attractors is further explored in section IV. Section V contains a detailed study of low free-energy TAP states obtained from studying the solutions using the ‘edge of chaos’ algorithm. Section VI concludes with a discussion and summary of the main results.

## II. SOLVING THE TAP AND NMF EQUATIONS BY ITERATION

The TAP and NMF equations can be derived from the following generalized free-energy function:

$$F = - \sum_{(i,j)} J_{ij} m_i m_j - \gamma \frac{\beta N}{4} (1-q)^2 + \frac{1}{\beta} \sum_i \left[ \frac{1+m_i}{2} \ln \frac{1+m_i}{2} + \frac{1-m_i}{2} \ln \frac{1-m_i}{2} \right] \quad (1)$$

where  $\gamma = 1$  corresponds to TAP and  $\gamma = 0$  to NFM. In Eq. (1) the local magnetizations,  $m_i = \langle S_i \rangle$ , lie in the range  $-1 \leq m_i \leq 1$ ,  $\beta = 1/kT$  as usual, and  $q = (1/N) \sum_i m_i^2$ .

The TAP and NFM equations themselves are derived from the equations  $\partial F / \partial m_i = 0$ ,  $i = 1, \dots, N$ , which give the turning points of  $F$ . They can be written in the form

$$m_i = \mathcal{G}_i(\vec{m}) = \tanh [\beta h_i - \gamma \beta^2 (1-q) m_i] \quad (2)$$

where the local field  $h_i = \sum_{j \neq i} J_{ij} m_j$ . The second term in the argument of the tanh function is, for the TAP case  $\gamma = 1$ , the Onsager reaction term. The TAP equations are exact as  $N \rightarrow \infty$  for the SK model. The naive mean-field equations are exact for the Wallace model, in which at each site  $i$  in the system there is a set of Ising spins  $s_{ia}$  ( $a = 1, 2, \dots, k$ ), each of which interacts with the  $k$  spins at sites which are coupled to the  $i$ -th site and the limit  $k \rightarrow \infty$  is taken [9].

The set of spins  $m_i$  that satisfy (2) can be thought of as a fixed point  $\vec{m}^*$  of the map

$$m_i^{(k+1)} = \mathcal{G}_i(\vec{m}^{(k)}) . \quad (3)$$

This map could be applied to all spins in parallel, to each spin separately and in sequence, each time to a random spin, or to a spin chosen for some particular reason. It turns out that for the NMF equations ( $\gamma = 0$ ), application of this map leads always to a fixed point that coincides with a minimum in the free energy landscape, no matter how the map is applied. This fact one establishes by calculating, at the fixed point, the Hessian  $H$  which is the matrix of second derivatives of the free energy,

$$H_{ij} = \left. \frac{\partial^2 F}{\partial m_i \partial m_j} \right|_{\vec{m}^*} = -J_{ij} - \gamma \frac{2\beta m_i^* m_j^*}{N} + \left[ \frac{1}{\beta} \frac{1}{1 - (m_i^*)^2} + \gamma \beta (1-q) \right] \delta_{ij}, \quad (4)$$

(which holds for all  $i, j$  if one takes  $J_{ii} \equiv 0$ ) and checking that all its eigenvalues are positive, thus defining a minimum. As we will see below, the free energy landscape also has turning points with a positive number  $K$  of negative eigenvalues—we call these saddle points of index  $K$ . On the other hand the inclusion of Onsager reaction term leads to the map (3) almost never converging on a fixed point.

Clearly one does not imagine that the trajectory described by iteration of the map (3) corresponds to any reasonable physical dynamics on the free energy landscape, e.g., a zero-temperature dynamics in which one follows the path of steepest descent to a local (in general, metastable) minimum. Unfortunately, numerical algorithms that one might expect to approximate closely a physical dynamics (such as steepest descents or conjugate gradients) turn out to be poorly adapted to the NMF free energy landscape. The reason for this is that the free energy minima tend to lie close to the sides of the hypercube  $-1 \leq m_i \leq 1$  over which the free energy is defined. Naively, one might imagine that the divergence in the free energy gradient as the hypercube's boundary is approached would prevent a descent algorithm from exiting the physical region. However, the weak and short-ranged logarithmic divergence is not resolved numerically. This can cause points to be reached that lie outside the hypercube and for which the free energy (1) is undefined, thereby creating an obvious numerical problem. We tried a number of modifications here to work around this, such as mapping the bounded hypercube to an infinite domain, or inventing a fictitious free energy outside the hypercube, all to no avail.

For this reason, we modified instead the iterative map (3) in a way that we believe gives some insight into the free energy minima located by a physical dynamics. This map reads

$$m_i^{(k+1)} = m_i^{(k)} + \alpha \left[ \mathcal{G}_i(\vec{m}^{(k)}) - m_i^{(k)} \right] \quad (5)$$

in which  $\alpha$  is a parameter that controls the speed of approach to the next iterate. We describe the utility of this more general iterative scheme first in the context of the NMF equations ( $\gamma = 0$ ) and then the TAP equations ( $\gamma = 1$ ).

### A. NMF Equations

If in Eq. (5) the parameter  $\alpha$  is small, one expects a smooth trajectory to be followed, and crucially one that is constrained to remain within the hypercube. This statement can be made more precise by noting that the displacement  $\delta m_i = \alpha(\tanh \beta h_i - m_i)$  is bounded:  $|\delta m_i| \leq 2\alpha$  and so can be made arbitrarily small by decreasing  $\alpha$ . Furthermore, one can show that the projection of this displacement onto the gradient vector of the free energy is always negative. Thus, for sufficiently small  $\alpha$ , the dynamics should take a small step in such a way as

$N$	Samples	Random	Cyclic	Greedy	Physical
20	2000	-0.67196(3)	-0.67151(3)	-0.67285(3)	-0.67211(3)
30	1000	-0.68811(4)	-0.68760(4)	-0.68882(4)	-0.68804(4)
40	1000	-0.69900(4)	-0.69862(4)	-0.69973(4)	-0.69892(4)

TABLE I: Average free energy of minima in the NMF free energy landscape reached using various iterative algorithms. For all system sizes  $N$ ,  $\beta = 2$  and different minima were located by restarting the algorithm for each sample from 5000 different, random initial conditions.

to lower the free energy, a fact that has been verified numerically. Although we do not claim that this dynamics is equivalent in any sense to a steepest-descent dynamics, the fact that the free energy is lowered in a controlled fashion leads us to view it as a ‘physical’ dynamics.

In Table I we display the free energy of the NMF minima located using four different algorithms, averaged over both a number of different realizations of the disorder (i.e., sets of the random variables  $J_{ij}$ , each of which we refer to as a *sample*) and over a number of different initial conditions on the iteration. So that the algorithms can be properly compared for a given system size  $N$ , each was treated to the same set of samples. The system sizes used were quite small ( $N = 20, 30, 40$ ) so that we may later compare with the exhaustive search for *all* turning points in the same samples (see Section III). The first three of the four algorithms are implementations of (3) applied on a spin-by-spin basis in different ways. In the *random* algorithm, the spin chosen for update is chosen at random, whereas in the *cyclic* algorithm, each is visited in order. Meanwhile, the spin chosen in the *greedy* algorithm is that for which the free energy will decrease the most under application of the map. Finally the *physical* algorithm uses (5) applied *simultaneously* to all spins and with the control parameter  $\alpha = 10^{-3}$ . We notice from the Table that the differences in the free energy arising from a change of algorithm, whilst significant compared to the errors, are about two orders of magnitude smaller than those arising from an increase in the system size. Later, we will provide evidence that these changes are also small on the scale of free energies spanned by all the solutions of the NMF equations.

### B. TAP Equations

Solutions of the TAP equations, i.e. (2) with  $\gamma = 1$ , are much harder to find than those of the NMF equations. Part of the reason for this is that including the Onsager reaction term stabilizes the trivial (paramagnetic) solution  $\vec{m} = 0$ . Indeed, when we employed simple-minded free energy minimization algorithms on the TAP free energy landscape, we found almost always this trivial solution. However, this solution is *thermodynamically* unstable in the spin glass phase [10] and so one must take steps to avoid it. One possibility, pursued elsewhere, is to use a

different free-energy function in the thermodynamically unstable region [11].

We succeeded in finding solutions of the TAP equations using the iterative map (5) in the regime where  $\alpha$  is *greater* than one. The reason why this choice is useful is that with  $\alpha \leq 1$  the iteration enters a limit cycle between points that are unrelated to the turning points of the TAP free energy landscape. By amplifying the displacements between these points, it is possible to break out of the limit cycle. An added bonus is that paths to the trivial solution  $\vec{m} = 0$  are also destabilized—this is because our observations suggest paths to this solution have an oscillatory character.

Clearly, there is an optimum value for  $\alpha$  for finding the largest number of solutions of the TAP equations. Too small, and the limit cycles are attractive; too large, and one may hop in great leaps about the hypercube, never to settle on a solution. As we shall see in Sec. V, the optimum  $\alpha$  is in fact close to a point where the iterative dynamics become chaotic. As this point is approached, the dynamics do exit the hypercube, but there are no numerical problems associated with this since the right-hand side of (5) is defined even if  $|m_i| > 1$ . We only require that the trajectory followed by the iteration converges on a fixed point inside the hypercube in a finite time. As we shall also later explain in detail, when  $\alpha$  is tuned to its optimum we can approach closely states with the thermodynamic equilibrium free energy.

### C. Preliminary Comparison of TAP and NMF

We believe that, despite having the same  $T \rightarrow 0$  limit as the TAP equations, solutions of the NMF equations will not take us to the lowest energy states. Unfortunately, since the equilibrium free energy of the NMF equations is not known exactly at finite temperature, we are unable to test whether it can be reached for this case. Instead, we probe the relationship between NMF free energy minima and low-lying states by performing a zero-temperature quench from the former. Specifically, having found a solution to the NMF equations, i.e., (2) with  $\gamma = 0$ , at finite temperature  $\beta$ , we then iterate the  $T = 0$  version of the map. That is, every spin is set to have unit magnitude but with the sign taken from the final state of the NMF iteration. Then, sites are visited randomly and flipped if they are not aligned with their local fields until a metastable state is reached in which all spins have become aligned with their fields. The energies of these states, averaged over different NMF turning points and different bond distributions, are shown in Fig. II C for a range of system sizes  $N$  and inverse temperatures  $\beta$ . A noticeable feature of the graph is that these energies have a nonmonotonic dependence on  $\beta$  and *increase* as the temperature is decreased past a certain point. This suggests that minima of the NMF free energy landscape (at least, those found by iterative methods) at low temperatures are far away from the low energy states. This

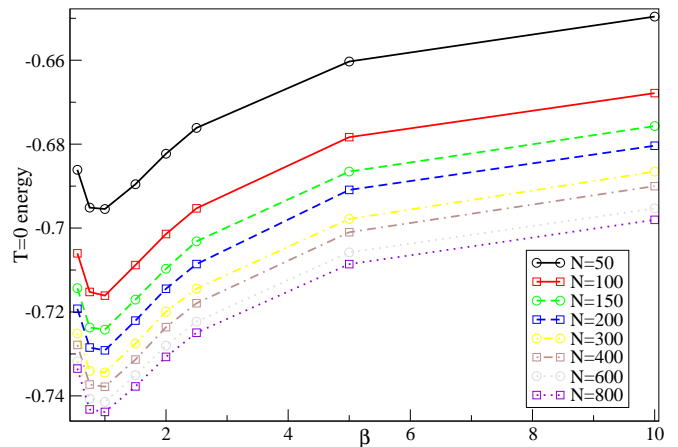


FIG. 1: Energies reached from solutions of the NMF equations found by iteration after a quench to a  $T = 0$  state at different system size  $N$  and inverse temperature  $\beta$ .

one sees from the fact that the lowest energy states obtained by this process occur at an apparently well-defined *finite* temperature  $\beta \approx 1$ .

A plausible explanation for the minimum is as follows. The total number of NMF solutions has the form  $\exp[N\Sigma(T)]$ , where  $\Sigma(T)$  is expected to be a monotonically decreasing function of  $T$ , vanishing at the critical temperature  $T_c = 2$  (where there is only one solution,  $m_i = 0$  for all  $i$ ). Exactly this behavior is obtained for the TAP equations [2], except that  $T_c = 1$  for TAP. It follows that, for any given system size  $N$ , there will be a range of temperatures near  $T_c$  where the condition  $N\Sigma(T) \ll 1$  will hold. In this regime there will be a unique solution with high probability. In fact there will be  $O(1)$  solutions down to a temperature  $T^*(N)$  defined by  $N\Sigma(T^*) = 1$ . For  $T > T^*$  the free energy will be determined essentially exactly, as there is only one solution. This state should provide a good starting point for the subsequent quench to  $T = 0$ . Our hypothesis, then, is that the minima in Figure II C occur at  $T \simeq T^*(N)$ . The relative insensitivity to  $N$  of the position of the minimum in Figure II C may be accounted for by the strong  $T$ -dependence of  $\Sigma(T)$  in the regime  $T > T_c/2$  (evident in the exact solution for TAP [2]).

As we have mentioned above, solutions of the TAP equations by (suitably chosen) iteration at the ‘edge of chaos’ can as  $T \rightarrow 0$ , yield states of the SK spin glass for which the energy per spin is close to the equilibrium value. We have also used an ‘edge of chaos’ algorithm for the  $T = 0$  version of the NMF equations and there too states of low free energy are obtained. However, the data presented in Fig. II C strongly suggests that this is not the case for the NMF equations when treated by an iterative procedure which parallels gradient descents. We believe that this is a consequence of the shape of the free energy landscape, which we shall now discuss. (For the TAP equations gradient descents algorithms usually fail to give any solution other than the trivial solution with

all  $m_i = 0$ ).

### III. THE SHAPE OF THE FREE ENERGY LANDSCAPE

In this section we investigate numerically some properties of the NMF free-energy landscape in order to contrast with a similar study of the TAP landscape presented in [6]. The strategy is to consider small systems and locate (as best one can) *all* the turning points in the landscape. We begin with a discussion of the numerical procedure.

#### A. Numerical method

In [6], turning points of the TAP free energy landscape were found using Broyden's method [12] for solving the system of nonlinear equations (2) with  $\gamma = 1$ . We found this algorithm also to be applicable to the case  $\gamma = 0$ , albeit in a different implementation [13]. Although more sophisticated and efficient root-finding algorithms exist, we found that they tended to fail for much the same reasons as did steepest descent and conjugate gradient methods for locating minima (as discussed above).

The numerical algorithm approaches a single root deterministically from an initial condition, so in order to find different roots, a sequence of random initial conditions were tried. One hopes that, after a sufficiently large number of initial conditions, one will have located each of the turning points in the NMF landscape at least once. One test that reveals if any solutions are certainly outstanding is to calculate the Morse sum

$$S_M = \sum_{i=1}^{N_{\text{solns}}} (-1)^{K_i} \quad (6)$$

where  $K_i$  is the saddle index (number of negative eigenvalues of the Hessian) of the  $i^{\text{th}}$  turning point. Topological considerations imply that  $S_M = 1$  when the sum is over all turning points of the NMF free energy. Hence, if one finds  $S_M \neq 1$ , there remain solutions to be found. The converse, however, is not true, and so one must use a little trial-and-error to estimate the typical number of initial conditions after which no new solutions are found.

Computational constraints imply a trade-off between temperature and system size. The larger the system size, the slower the search for a single solution and if one works at too high a temperature, this fact places too low a limit on the typical number of turning points per sample that can be located in a reasonable time. Conversely, at too low a temperature, the number of solutions per sample grows so fast with system size that one is unable to survey effectively a reasonable range of system sizes. We found an agreeable compromise occurred at  $\beta = 2$  (the critical point in NMF is  $\beta_c = 1/2$ ) which allowed the study of samples up to size  $N = 40$ . At this system size there were typically 600 turning points per sample, compared with

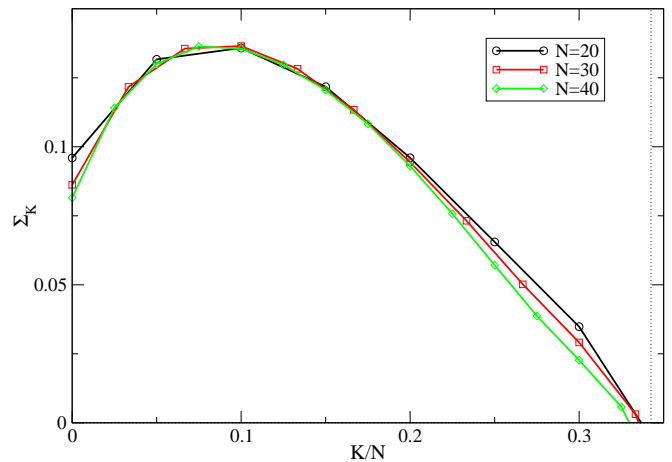


FIG. 2: Complexity  $\Sigma_K$  of the NMF equations with solutions separated according to the index of the saddle  $K$ . Near the peak, the data collapse when  $K$  is scaled by  $N$  for  $N = 20, 30, 40$  at  $\beta = 2$ . The dotted line corresponds to the index of the trivial solution in the thermodynamic limit.

45 at  $N = 20$ . Whilst the criterion  $S_M = 1$  was satisfied for all but a handful of 2000 samples with  $N = 20$  sites, it held only for about a third of the 1000 samples at  $N = 40$ . The data presented in the following are obtained by amalgamating results from *all* samples, including those whose solution sets were certainly incomplete by virtue of  $S_M \neq 1$ . Excluding these samples from the analysis changes our results very little.

#### B. Results

We first examine what classes of turning point arise in the free-energy landscape. In the TAP free energy landscape, one finds only minima and index  $K = 1$  saddles which occur in pairs (so that, along with the trivial solution, the Morse sum is satisfied) [5, 6]. From an analysis of all the minimum-saddle pairs for small systems, Cavagna *et al.* [6] find that the free energy difference between a minimum and its corresponding saddle point seems to vanish in the thermodynamic limit.

For the NMF equations we find minima and saddles of *all* indices up to some maximum that grows linearly with system size. This result is best illustrated using the *saddle complexity*  $\Sigma_K$ , defined as

$$\Sigma_K = \frac{\ln N_{\text{solns}}(K)}{N} \quad (7)$$

in which  $N_{\text{solns}}(K)$  is the number of solutions of the NMF equations that correspond to a saddle point of index  $K$ . Rescaling  $K$  with  $N$  one obtains Fig. 2 which shows a good collapse around the peak that occurs at  $K \approx 0.1N$ .

A little more insight is gained into the shape of the free energy landscape by plotting for a given saddle index  $K$  the complexity as a function of free energy—see Fig. 3 for

the case  $N = 40$ . Here one sees a set of roughly similarly-shaped curves with a well-defined maximum at a free energy that increases with  $K$  whilst the width of the curves decreases. This suggests that the highest-energy turning points are also the most unstable, and a closer inspection of the data reveals that the trivial solution seems always to have the greatest index.

To determine the value of  $K/N$  of the trivial solution in the thermodynamic limit, we need to find the total density of negative eigenvalues of the Hessian matrix  $H$ , which from (4) is, at  $\vec{m} = 0$  (and  $\gamma = 0$  for NMF),

$$H_{ij} = -J_{ij} + \frac{1}{\beta} \delta_{ij}. \quad (8)$$

In this expression,  $J$  is a symmetric Gaussian random matrix, and one can appeal to the Wigner semicircle law to learn that, in the limit  $N \rightarrow \infty$ , its eigenvalues  $\lambda$  have a distribution

$$\rho_J(\lambda) = \frac{1}{2\pi} \sqrt{4 - \lambda^2} \quad (9)$$

on the support  $-2 \leq \lambda \leq 2$ . Clearly, the diagonal part of  $H$  serves simply to shift the distribution to the right by  $1/\beta$  and so the number  $K$  of the  $N$  eigenvalues that are negative has the limit

$$\lim_{N \rightarrow \infty} \frac{K}{N} = \frac{1}{2\pi} \int_{-2+1/\beta}^0 d\lambda \rho_J(\lambda - 1/\beta) \quad (10)$$

$$= \frac{1}{2} - \frac{1}{\pi} \arcsin \frac{1}{2\beta} - \frac{1}{4} \sqrt{4 - \frac{1}{\beta^2}}. \quad (11)$$

For  $\beta < 1/2$  we see that the trivial solution has no negative eigenvalues, i.e., we are above the critical temperature for the spin glass phase. For the case  $\beta = 2$  studied numerically, the fraction of negative eigenvalues approaches  $K/N \approx 0.3425$ , which is plotted as a vertical dotted line in Fig. 2. We note that even for the small systems studied, the complexity approaches zero at this value. (Actually, in these finite systems, we obtained solutions with larger index but their complexity was negative—i.e. there was on average fewer than one such solution per sample—and hence irrelevant in the thermodynamic limit).

More generally, one can look at the distribution of eigenvalues of the Hessian at other turning points. In Fig. 4 these are shown for the  $N = 40$  system, averaged over all turning points and also separated out into the average distributions at minima and saddles of index  $K = 1$  and 2. Most noticeable is a dip in *all* the spectra around  $\lambda = 0$ . We believe this is a real effect and not an artifact of the numerics: the plots for  $N = 20$ —where we are confident that all the turning points in the free energy landscape have been isolated—show the same behavior. We are however, currently unable to explain this repulsion of low-eigenvalue modes of the Hessian.

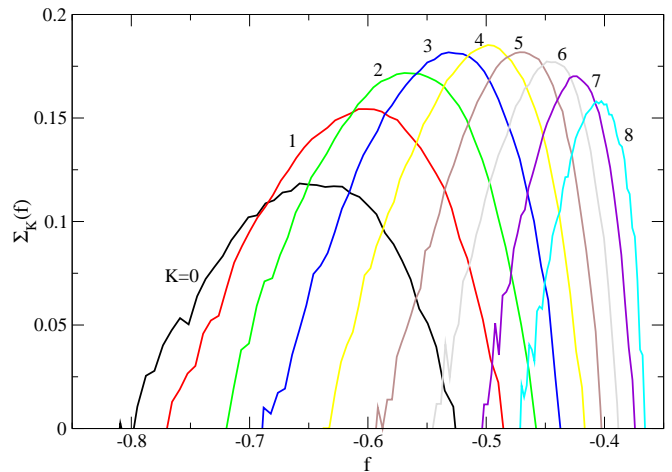


FIG. 3: Complexity  $\Sigma_K(f)$  of the NMF equations as a function of free energy  $f$  for different saddle index  $K$ , system size  $N = 40$  and  $\beta = 2$ .

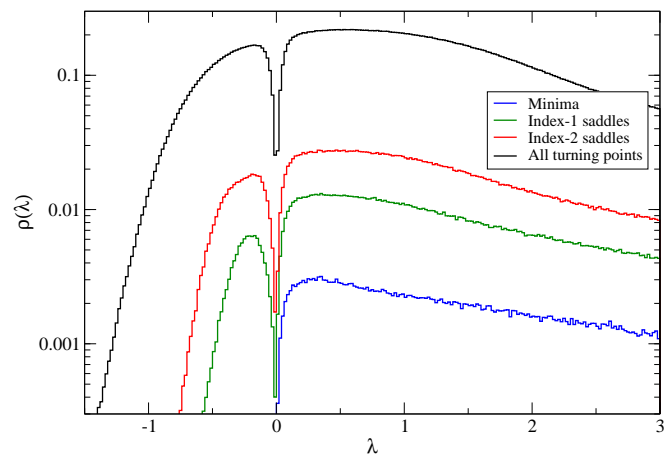


FIG. 4: Eigenvalue distributions of the Hessian at minima, saddles of index 1 and 2 and all turning points. The system size  $N = 40$  and  $\beta = 2$ . Note that the vertical scale is logarithmic.

#### IV. CONNECTION BETWEEN ITERATIVE SOLUTIONS AND THE STRUCTURE OF THE FREE-ENERGY LANDSCAPE

We now move on to discuss how the structure of the free energy landscape influences (if at all) the attractors of the iterative maps described in the previous section. In the foregoing, we showed that for the NMF equations, the typical free energies of turning points of a particular type increase with the saddle index  $K$ . In particular, there is a free energy at which, when approached from above, the number of minima exceed the number of saddle points. Recall, in fact, that the complexity describes the *exponential* increase of the number of solutions with system size, so that below this characteristic free energy the ratio of the number of saddle points to minima vanishes in the thermodynamic limit. In Fig. 5 we plot the

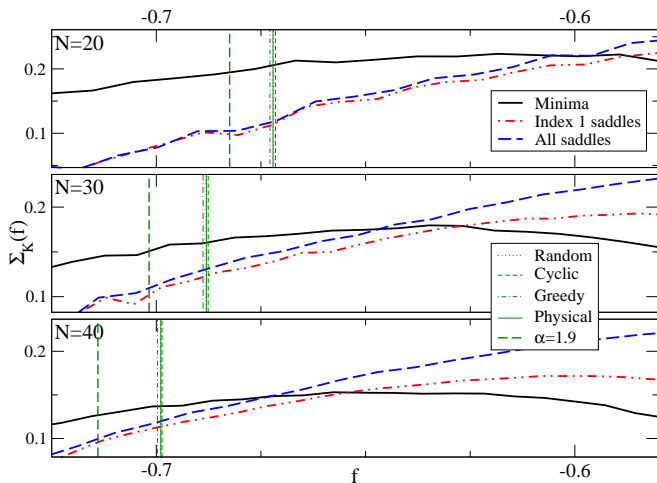


FIG. 5: Complexity  $\Sigma_K(f)$  of the NMF equations as a function of free energy  $f$  for three classes of turning point (minima,  $K = 1$  saddles and all saddles) and system sizes  $N = 20, 30, 40$ , all at  $\beta = 2$ . For comparison, the mean free energies of states found by the various iterative algorithms are plotted. All the energies cluster together except for those obtained by the ‘edge of chaos’ algorithm i.e. Eq. (5) with  $\alpha = 1.9$ , which outperforms them by a considerable margin.

mean free energies set out in Table I for the various iterative algorithms alongside the corresponding complexity histograms for minima,  $K = 1$  saddles and all saddles for the three system sizes  $N = 20, 30, 40$ .

We first notice that the spread in free energies within the different iterative algorithms (indicating a slight bias of the algorithms towards different attractors) is small compared to the free-energy range spanned by a set of turning points (the minima, say). Noting that all three plots in Fig. 5 have the same horizontal scale, it is clear that as  $N$  increases, the mean free energy located by the iterative algorithms approaches the largest free energy at which the minima start to outnumber the saddles. Of course, since we have been unable to access larger system sizes this provides no proof that these points will coincide as  $N \rightarrow \infty$ ; however, this data provides support for a ‘landscape’ picture of zero-temperature dynamics in which the free energy is lowered until such time as the minima dominate to such an extent that becoming trapped in a local minimum is an inevitability. Notice that in the ‘saddles rule’ type of hypothesis [14] the dynamics is supposed to be trapped at the value of the free energy at which the index density  $k(f) = \langle K \rangle / N$  becomes non-zero, where the average is over all solutions whose free energy lies between  $f$  and  $f + df$ . We have plotted this quantity in Fig. 6. Clearly for the system sizes which we have been able to study the free-energy per spin of most algorithms is of order  $-0.69$  (see Table I). This is much higher than the value of  $f$  at which  $k(f)$  appears to become non-zero. But the number  $-0.69$  does seem to fit better with the free energy at which index 1 saddles begin to outnumber the index 0 saddles i.e.

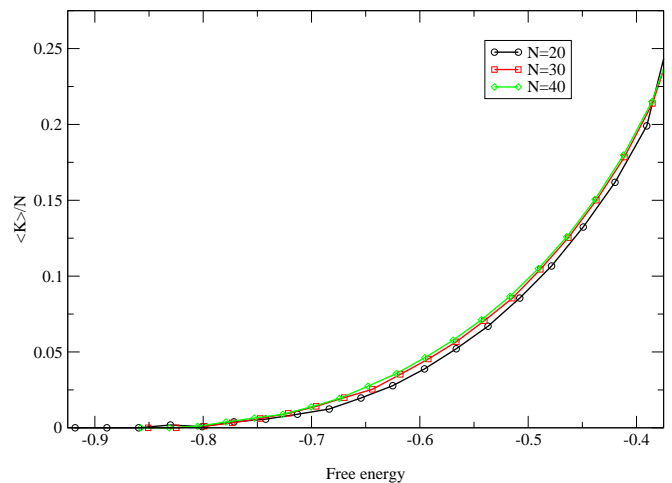


FIG. 6: Index density of the NMF equations as a function of free energy  $f$  at  $\beta = 2$  and system sizes  $N = 20, 30, 40$ .

the minima, so perhaps a modified version of the ‘saddles rule’ hypothesis does apply to the NMF landscape.

As mentioned above, the TAP free-energy landscape contains exponentially large (in  $N$ ) numbers of minima and  $K = 1$  saddles *only*. Not only that, but these turning points come in pairs, i.e., a minimum that is close to a saddle in the sense that it is separated by a total free energy difference that vanishes approximately as  $N^{-0.26}$  in the limit  $N \rightarrow \infty$  [6]. What this means in particular is that for the TAP equations the complexity of minima  $\Sigma_0(f)$  and of  $K = 1$  saddles  $\Sigma_1(f)$  are *equal* for all free energies  $f$  (and all other complexities are zero). Therefore there is no ‘crossing point’ at which minima begin to outnumber saddles as there is for the NMF equations. Since the solutions we found are compatible with tracking down states of lower free energy, it would appear that the fact that there are equal numbers of saddles and minima over a range of free energy means that one does not get trapped in a particular minimum, but somehow manages to explore further the free energy landscape by passing over the nearby saddle-point. This latter statement is, however, as yet somewhat speculative and requires further investigation.

## V. DYNAMICAL PROPERTIES OF THE TAP ITERATION

As mentioned previously, the TAP equations are usually very difficult to solve numerically. However, using the modified map Eq. (5) with  $\alpha > 1$  surprisingly leads to a vastly increased probability of finding solutions. In this section we explain in more detail why this is the case and how the *ad hoc* parameter  $\alpha$  should be chosen for optimal results. First, however, we discuss the details of the implementation as there are a number of potential pitfalls.

### A. Numerical iteration

The iteration Eq. (5) is best applied to each spin separately and in sequence to improve convergence. At low temperatures the converged result usually contains some  $m_i$  which are equal to  $\pm 1$  within numerical accuracy. While this might be considered merely an irrelevant numerical inaccuracy, it is a serious problem as soon as the Hessian, Eq. (4), of the solution is required as it is clearly ill-defined if  $m_i = \pm 1$ . Therefore we continue iteration of a transformed version of the TAP equations for the variables  $x_i = -\text{sign}(m_i) \ln(1 - m_i^2)$ ,

$$x_i^{(k+1)} = x_i^{(k)} + \alpha \left[ 2\mathcal{H}_i + 2\text{sign}(\mathcal{H}_i) \ln \frac{1 + e^{-2|\mathcal{H}_i|}}{2} - x_i^{(k)} \right], \quad (12)$$

where  $\mathcal{H}_i = \tanh^{-1} \mathcal{G}_i$ . This particular choice of transformed variables is adapted to the form of the Hessian, Eq. (4). The diagonal elements of  $H_{ij}$  can be obtained from  $|x_i|$  simply by exponentiation without fear of numerical overflow or loss of accuracy. The initial condition for the iteration of the transformed variables is obtained from the set of converged  $m_i$  via  $x_i^{(0)} = 2\mathcal{H}_i + 2\text{sign}(\mathcal{H}_i) \ln \frac{1 + e^{-2|\mathcal{H}_i|}}{2}$  applied to all spins in parallel. This is important since application in sequence would implicitly carry out more iteration steps and would not result in an accurate translation of the  $m_i$  into the transformed variables  $x_i$ , thus in practice often leading to exit from the basin of attraction.

When convergence is reached using the transformed variables, the Hessian is calculated. Diagonalization of it is, however, hampered by its severe ill-conditionedness, particularly at low temperatures. The eigenvalues may vary over 100 orders of magnitude, owing to the extremely large variation of the diagonal entries. Therefore standard diagonalization packages fail and one has to resort to, e.g., diagonalization routines from [15] modified for use with arbitrary precision packages such as [16].

### B. Dynamical critical point

The fact that iterations with  $\alpha > 1$  generally find many solutions of the TAP equations and iterations with  $\alpha \leq 1$  basically never find solutions (other than the trivial one) suggests that  $\alpha = \alpha_c = 1$  is a critical point of the iterative dynamics. Just as the iterative behavior of e.g. the logistic map is changed from convergence to a stable fixed point to eventually chaotic dynamics via its control parameter, we expect that we have stable fixed points for  $\alpha > 1$  and chaotic behavior for  $\alpha \leq 1$ . We test this hypothesis by various means. First we analyze scaling properties which we expect to hold near the critical point. We then examine the lengths of limit cycles above and below the critical point.

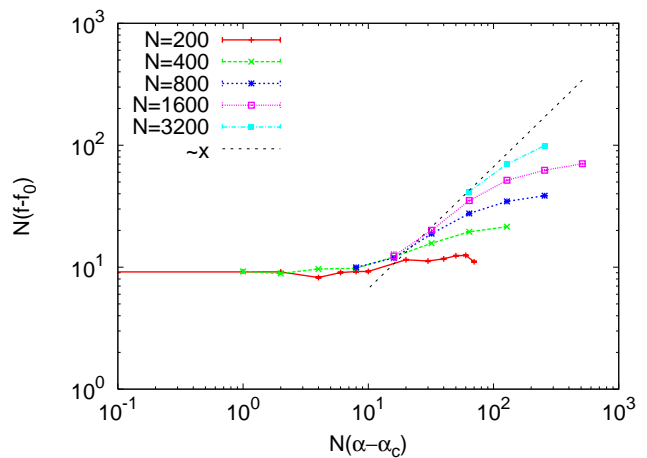


FIG. 7: Finite-size scaling of the free energy as a function of the scaling variable  $x = N(\alpha - \alpha_c)^\gamma$ , with  $\gamma = 1$ , at inverse temperature  $\beta = 20$ .

### C. Scaling properties near the critical point

The choice of the parameter  $\alpha$  is not arbitrary. A given value of  $\alpha$  favors finding a particular subset of all solutions, i.e. the typical free energies found are correlated with  $\alpha$ . Under the hypothesis of the existence of a critical point at  $\alpha = \alpha_c = 1$  the free energies  $f$  obtained with a given  $\alpha$  are hypothesized to obey a finite-size scaling form

$$f - f_0 = N^{-1} F(N(\alpha - \alpha_c)^\gamma), \quad (13)$$

where  $f_0$  is the exact free energy per spin in the thermodynamic limit, which is known exactly from methods described in [17, 18] to be  $f_0 \approx -0.76324 \dots$  at  $\beta = 20$  [19]. Fig. 7 shows the connection between  $\alpha$ , the system size  $N$  and the average free energy  $f$  of the solutions found at inverse temperature  $\beta = 20$  in a finite-size scaling plot with scaling variable  $x = N(\alpha - \alpha_c)^\gamma$ . The best data collapse is obtained for an exponent  $\gamma \approx 1$ , but with too much scatter to provide an error bar. The finite-size corrections are still very large, as can be seen from the deviations at large arguments. The scaling function  $F(x)$  seems to behave as  $x^\eta$  for large  $x$  with  $\eta \approx 1$ . This would imply that, away from the critical point, the excess free energy per spin approaches an algorithm-dependent (here  $\alpha$ -dependent) value, in accordance with a result of Newman and Stein [20] which states that, in the thermodynamic limit, any given algorithm for solving the TAP equations will find solutions of a given free energy per spin, characteristic of the algorithm. In our case any fixed choice of  $\alpha$  defines an algorithm and the scaling form with  $\eta = 1$  then gives  $f = f_0 + \text{const.}(\alpha - \alpha_c)$  for  $N \rightarrow \infty$ , as required. In the opposite limit, the data suggest  $F(0) = \text{const.}$ , i.e. for  $\alpha \rightarrow \alpha_c$ , the excess free energy *per spin* vanishes.

As a spin-off of these results we therefore deduce that using the modified map Eq. (5) we can, in principle, find



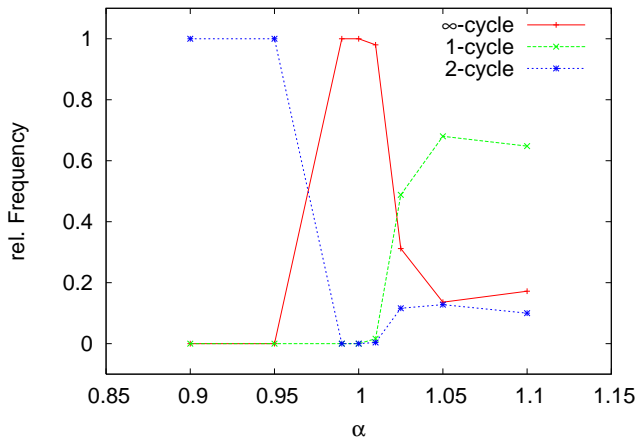


FIG. 8: The data from Tab. II plotted for lengths 1, 2, and  $\infty$

states with free energy per spin arbitrarily close to  $f_0$  by choosing the scaling variable  $x = N(\alpha - \alpha_c)^\gamma$  as small as possible. The drawback is that the probability of finding any solutions at all goes to zero as  $\alpha \rightarrow \alpha_c$ . This will be illustrated in the following two subsections.

#### D. Cycle lengths

As  $\alpha$  is decreased, limit cycles in the dynamics occur with increasing frequency. In order to further test the hypothesis that  $\alpha = 1$  is a critical point we have calculated the lengths of limit cycles as a function of  $\alpha$ . Table II and Fig. 8 show the frequency with which limit cycles of a given length were found for 10 samples of an  $N = 800$  system at  $\beta = 20$  using 25 different random starting positions each. We checked for limit cycles up to length 20 beyond which they were considered to be infinitely long. There is a marked change from  $\alpha = 1.1$ , where 65% of the starting positions lead to convergence (i.e. a limit cycle of length 1), to  $\alpha = 1$ , where 100% of the starting positions did not run into a limit cycle (of length less than 20) at all. There is another very distinct change between  $\alpha = 0.99$  and  $\alpha = 0.95$  from infinite limit cycles to cycles of length 2. Closer inspection revealed that these latter cycles are of the form  $m_i \rightarrow -m_i \rightarrow m_i$ .

The picture which emerges from this data is that for  $\alpha > 1$  we find a distribution of cycle lengths which includes a finite fraction of cycles with length 1, i.e. convergence. When  $\alpha$  is tuned towards 1, more and more weight is taken from the finite limit cycles and transferred to the infinite one, until at  $\alpha = 1$  all cycles have infinite length. At the same time, decreasing  $\alpha$  towards the value one leads to states with ever lower free energies. The optimum results for the free energy (giving the equilibrium free energy per spin in the thermodynamic limit) seemingly occur when the system is ‘at the edge of chaos’. Similar ideas have put forward in a recent paper

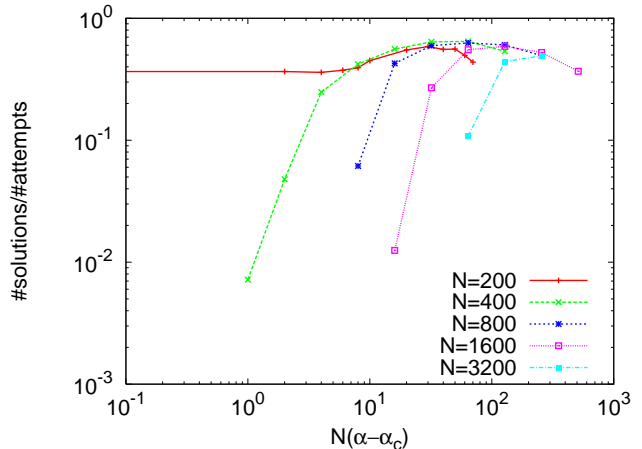


FIG. 9: Success rates (probability of finding a solution) as a function of the scaling variable  $N(\alpha - \alpha_c)$ .

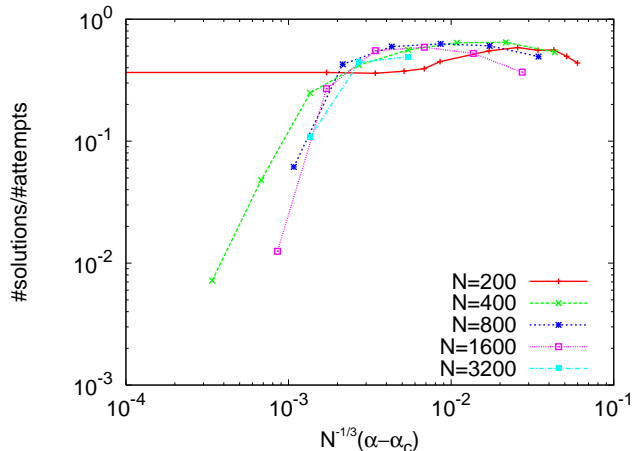


FIG. 10: Success rates as a function of  $N^{-1/3}(\alpha - \alpha_c)$ .

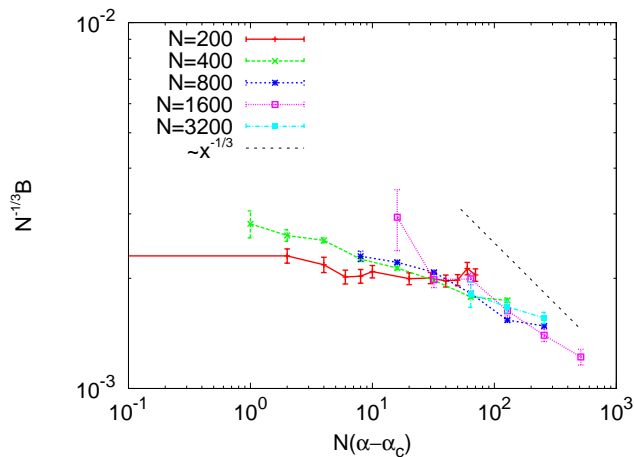
by Boettcher and Frank [8], who refer to ‘optimizing at the ergodic edge.’

#### E. Success rates

The probability of finding cycles of length 1, i.e. convergence, is not only a function of  $\alpha$  but, naturally, also of the system size  $N$ . While the scaling of the free energy in Fig. 7 suggests that by tuning  $\alpha$  towards 1 solutions of arbitrarily low free energy can in principle be found, we will now show that in practice this becomes increasingly difficult for large system sizes. Fig. 9 shows the success rates (probability of convergence to a solution from a random starting position) for various system sizes. The larger the system is, the more attempts are needed to find a solution. This statement can be made more precise by plotting the success rates against  $x' = N^{-1/3}(\alpha - \alpha_c)$ , which is done in Fig. 10. It shows that, at least for system sizes  $\geq 800$ , the success rates fall on a master curve

TABLE II: Frequency of appearance of limit cycles of a given length. The system size is  $N = 800$  at temperature  $\beta = 20$ .

$\alpha$	Length of limit cycle									
	1	2	3	4	5	6	7	8	9	$\infty$
1.1	0.648	0.1	0,048	0,02	0.004	0	0	0.004	0.004	0.172
1.05	0.68	0.128	0.012	0.028	0.004	0	0.004	0.004	0.004	0.136
1.25	0.312	0.116	0.012	0.04	0.008	0.016	0.004	0.004	0	0.488
1.01	0.016	0.004	0	0	0	0	0	0	0	0.98
1.0	0	0	0	0	0	0	0	0	0	1
0.99	0	0	0	0	0	0	0	0	0	1
0.95	0	1	0	0	0	0	0	0	0	0
0.9	0	1	0	0	0	0	0	0	0	0

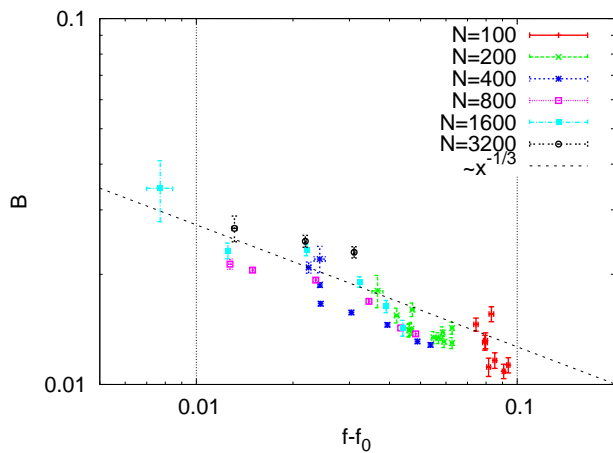
FIG. 11: Finite-size scaling of the barrier height as a function of the scaling variable  $x = N(\alpha - \alpha_c)$  at inverse temperature  $\beta = 20$ .

which goes to zero very quickly (faster than a power, and consistent with a Lifshitz-like behavior  $\sim e^{-\text{const.} \times x'^{-\zeta}}$  with  $\zeta \approx 2$ ) for small arguments.

So while the appropriate scaling variable is  $x = N(\alpha - \alpha_c)$  for the free energies and barrier heights (see below), it is  $x' = N^{-4/3}x$  for the success rates. Fixing  $x$  and thus a preferred range of free energies drastically reduces the success rates for large systems. Assuming a Lifshitz tail as suggested above, the success rates are proportional to  $e^{-\text{const.} \times N^{4\zeta/3}}$ .

## F. Barrier heights

Since minima and saddles of index 1 always occur in pairs in the TAP landscape [5], the barrier height of a solution can be defined as the free energy difference between a minimum and its corresponding saddle. Fig. 11 shows a scaling plot of the barrier heights using the same scaling variable as in Fig. 7. The data collapse is not very good, but is consistent with a barrier height exponent  $\psi = 1/3$ , which is the expected scaling for the SK

FIG. 12: The (total) barrier height as a function of free energy (per spin). Each data point represents the average over all solutions found with a particular value of  $\alpha$ .

model [21]. This suggests that the barriers between very low-lying minima and their corresponding saddles, with free energies per spin equal to the equilibrium value, scale as  $N^{1/3}$  for large  $N$ , but with a rather small coefficient of order  $10^{-3}$ . For larger values of the scaling variable, where the free energy per spin lies above the equilibrium value (see Fig. 7), the barriers decrease. The straight line in Fig. 11 has a slope  $-1/3$ , so if the data were to follow this line it would indicate that the barriers become  $N$ -independent at higher free energies. Recall that the barriers averaged over *all* TAP states were found to actually decrease with  $N$ , roughly as  $N^{-0.26}$  [6]. It should be noted, however, that the states of a given free energy reached by our particular algorithm almost certainly do not sample *all* states of that free energy uniformly.

The scaling behavior of the excess free energy per spin and of the barrier heights for large argument  $x = N(\alpha - \alpha_c)$ , namely  $f - f_0 \sim x$  and  $N^{-1/3}B \sim x^{-1/3}$ , indicates that (at least for large  $x$ ) the barrier height is directly proportional to  $(f - f_0)^{-1/3}$  with no dependence on  $N$  or  $\alpha - \alpha_c$ . Fig. 12 demonstrates that surprisingly this is not only true for large  $x$  but for *all* values of  $N$  and

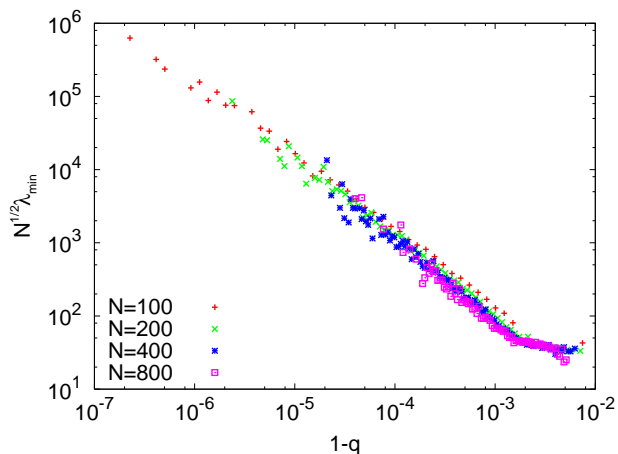


FIG. 13: Finite size scaling plot of the average smallest eigenvalue  $\lambda_{\min}(q)$  of the Hessian at a minimum versus  $1 - q$ . The eigenvalues scale with  $N^{-1/2}$ . The data shown is for  $\alpha$  such that the scaling variable is a constant, namely  $N(\alpha - \alpha_c) = 16$ .

$\alpha - \alpha_c$  explored. This is an important result since the dependence on the unphysical  $\alpha$  has been eliminated and the relation  $B \sim (f - f_0)^{-1/3}$  is a property of physical quantities alone.

### G. Eigenvalues of the Hessian

According to our picture of the TAP landscape described in [5], the Hessian at a minimum should, in the thermodynamic limit, have one null eigenvalue and a band of eigenvalues starting at a value strictly larger than zero. In order to confirm this, we have studied the eigenvalues of the Hessian at the solutions found by our algorithm. Since the arbitrary-precision diagonalization is forbidding for large system sizes, we are restricted to  $N \leq 800$ . In the range of accessible system sizes we find a huge variation in the smallest eigenvalue  $\lambda_{\min}$  (see Fig. 13) which is at first sight contradicting our landscape picture. However, the eigenvalues  $\lambda_{\min}$  show a strong correlation with the corresponding value of  $q$  at the minimum. This is understandable from the form of the Hessian, Eq. (4) since the smallest eigenvalue will be of the same order of magnitude as the smallest diagonal entry of  $H_{ij}$ , which is proportional to  $1/(1 - m_{\min}^2)$  ( $m_{\min}$  being the  $m_i^*$  closest to 0). Therefore, for  $q$  very close to 1,  $\lambda_{\min} \sim 1/(1 - m_{\min}^2) \sim 1/(1 - q)$ . Fluctuations of  $q$  towards 1 will therefore cause great fluctuations in  $\lambda_{\min}$ . In the thermodynamic limit,  $q$  should be self-averaging, therefore the variations in  $\lambda_{\min}$  become small and our observation merely indicates the enormous finite-size corrections still present at our accessible system sizes.

The correlation between  $\lambda_{\min}$  and  $q$  and the strong variation of  $\lambda_{\min}$  over several orders of magnitude indicate that a simple average of  $\lambda_{\min}$  might not be very informative. Instead we consider the average  $\overline{\lambda_{\min}(q)}$  of

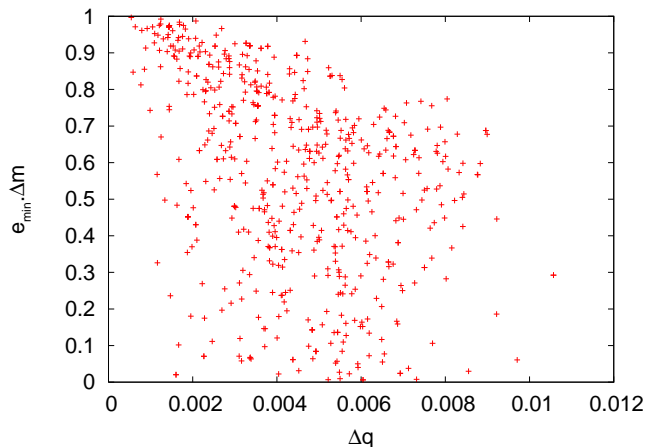


FIG. 14: Overlap between the eigenvector  $e_{\min}$  of the Hessian belonging to the smallest eigenvalue and the normalized difference vector  $\Delta m$  between a minimum and the corresponding saddle as a function of  $\Delta q = |q_{\text{saddle}} - q_{\min}|$ . The data are for  $N = 800$  at  $\beta = 20$  and  $\alpha = 1.02$ .

the eigenvalues as a function of  $q$ . This quantity is plotted in Fig. 13 in a finite size scaling plot which shows good data collapse, in particular for larger  $N$ . There are several points to notice in this figure. First, the eigenvalues scale with  $N^{-1/2}$  but can still be very large (of the order 1000 or more at the very low temperature,  $\beta = 20$ , at which we are working). Second, for larger  $N$  the range of  $q$ -values shrinks. This must be the case as in the thermodynamic limit there should be only one value of  $q$ . Third, the range of  $\lambda_{\min}$  also shrinks and  $\overline{\lambda_{\min}}$  (where the average now includes all values of  $q$ ) goes to zero as  $N^{-1/2}$  (note that it would have been very difficult to obtain this result from a simple  $q$ -independent average of  $\lambda_{\min}$ ). This is in support of the picture of the TAP free energy landscape outlined previously [5] which asserts that minima and saddles occur in pairs which move closer together as the system size grows. The smallest eigenvalues of the Hessian therefore have to go to zero with increasing  $N$ .

In order to provide further support for this picture, we have plotted in Fig. 14 the overlap between the eigenvector  $e_{\min}$  belonging to the smallest eigenvalue and the normalized difference vector (in  $m$ -space) between the minimum and its corresponding saddle  $\Delta m$ , as function of the difference  $\Delta q = |q_{\text{saddle}} - q_{\min}|$ . If the two vectors were uncorrelated, the distribution of their overlaps would be sharply peaked around zero. The figure shows, however, that they are strongly correlated and that the direction of the smallest eigenvector coincides with the direction in which the corresponding saddle is found. The correlation is particularly strong for small differences of  $q$  between saddle and minimum since these pairs are very close together.

The second smallest eigenvalue  $\lambda_2$  is expected to be, in the thermodynamic limit, strictly larger than 0. In order to test this, we have plotted in Fig. 15 the difference

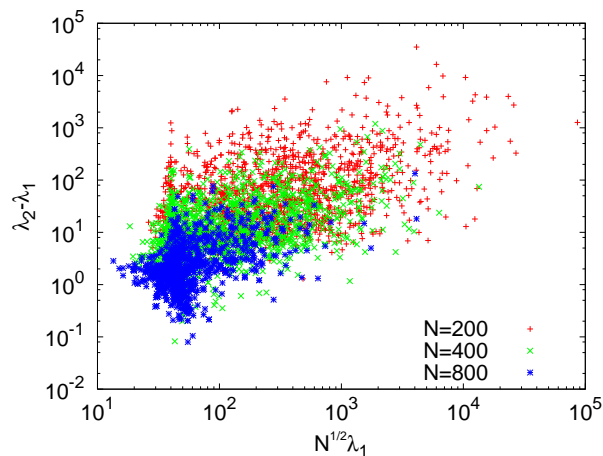


FIG. 15: Plot of the difference between the second and the lowest eigenvalue as a function of  $N^{1/2}\lambda_{\min}$ .

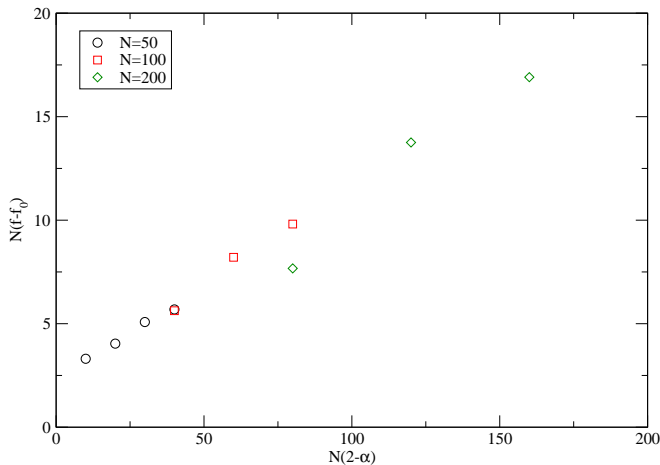


FIG. 16: Finite-size scaling of the NMF free-energy at  $T = 0$  as a function of the scaling variable  $x = N(2 - \alpha)$ .

between  $\lambda_2$  and  $\lambda_{\min}$  as a function of  $N^{1/2}\lambda_{\min}$ . In the thermodynamic limit there should be only a horizontal line of finite width in this plot. Clearly we are still very far away from this limit, even for  $N = 800$ , the variation in  $\lambda_2 - \lambda_{\min}$  being of order 10 or more. However, it is also clear that the data becomes more and more concentrated for larger  $N$ . Observe also the emergence of a horizontal line for  $N = 800$ .

## VI. DISCUSSION AND SUMMARY

In this work we have compared and contrasted the free-energy landscapes of two closely related models, described by the TAP equations and the NMF equations respectively. The TAP free-energy surface has a simple structure with turning points of only two types — minima, and saddle points of index 1. Furthermore, the minima and saddle-points occur in pairs, each containing

a minimum and a saddle point that are close neighbors in configuration space. By using a novel algorithm controlled by a single parameter  $\alpha$ , we are able to access TAP states whose free energy per spin is equal to the *equilibrium free energy per spin* at the given temperature, with an excess *total* free energy of order 10 (see Fig. 7). This is achieved by choosing the parameter  $\alpha$  close to a critical value,  $\alpha_c$ , beyond which the iterative dynamics becomes chaotic. The dependence of the excess total free energy  $\Delta F$  on  $N$  and  $\alpha$  is broadly consistent with a scaling form  $\Delta F = F[N(\alpha - \alpha_c)^\gamma]$ , valid in the limit  $N \rightarrow \infty$ ,  $\alpha \rightarrow \alpha_c$  with  $N(\alpha - \alpha_c)^\gamma$  fixed, and  $\gamma \approx 1$ . The scaling function  $F(x)$  should behave as  $F(x) \sim x$  for large  $x$ , so that  $\Delta F$  becomes of order  $N$  away from the critical point, while  $F(0)$  is a non-zero constant.

We have also studied the free-energy barriers, given by the free-energy difference between a minimum and its corresponding saddle point. In the low free-energy regime where  $N(\alpha - \alpha_c)^\gamma \ll 1$ , the barriers seem to grow as  $N^{1/3}$ , albeit with a small coefficient, while for  $N(\alpha - \alpha_c)^\gamma \gg 1$  we expect the barriers to be of order unity or smaller (see Fig. 11). This leads to a picture where only the lowest free energy states (with free energies per spin equal to the equilibrium one) are separated by barriers which increase in some manner with  $N$ .

In contrast to the TAP free-energy function, the NMF free energy has saddle points with index  $K$  taking values up to order  $N$ . The separate complexities  $\Sigma_K(f)$  have been computed numerically (see Fig. 3). The free energy at which the minima start to outnumber (exponentially in  $N$ ) the saddle points seems to play the role of a threshold free energy which acts as lower bound on the free energy that is dynamically accessible (Fig. 5).

We conclude with with some general remarks concerning optimization problems. If one is faced with a combinatorial optimization problem, such as finding the ground state of a spin glass, one approach is to write down TAP-like equations and solve them using an iterative scheme which is related to a descent procedure on the free-energy landscape. As the temperature is lowered the states obtained approach those of a zero-temperature problem. In the spin-glass context, it does not seem to matter, *a priori*, whether the finite-temperature generalization of the problem is through the TAP equations or the NMF equations, since they become identical at  $T = 0$ . We believe, however, that the very different structures of the free-energy landscapes in the two models will make a very big difference in practice. While the NMF free-energy surface is ‘robust’, with its threshold free energy and, presumably, large free energy barriers between states, the TAP free energy surface may be termed ‘fragile’. With any such problem therefore, it will pay to construct finite-temperature equations corresponding to a free energy with a fragile structure. This process might be called ‘sculpting the free-energy landscape’.

Finally we would like to point out that using algorithms which take one off the free-energy surface into physically unreachable regions before reaching the final

physical fixed point may also have great utility, as illustrated by our ‘edge of chaos’ algorithm. The success of this type of algorithm seems to be partly due to the fact that by allowing unphysical values of the  $m_i$  one can tunnel through barriers and partly because tuning the adjustable parameter  $\alpha$  towards the edge of chaos yields the solutions of low free energy which tend to be surrounded by the highest barriers which can trap the algorithm into a fixed point solution. We mainly used the ‘edge of chaos’ algorithm in connection with solving the TAP equations but it seems to work well also for the NMF equations. In Fig. 5 we have included the results obtained by setting  $\alpha = 1.9$  which is close to the ‘edge of chaos’ but without attempting to tune it to its optimum value for each value of  $N$ . (For the NMF equations the edge of chaos seems to be close to 2 and the values of  $\alpha$  which give stable solutions are less than the critical value). It is clear that it outperforms the other iterative algorithms, which approximate to descents on the free-energy surface, by a considerable margin. At  $T = 0$  the algorithm is especially simple and Fig. 16 shows that it seems to work as efficiently as the ‘edge of chaos’ algorithm applied to the TAP equations at low temperatures. However, it does suffer from similar problems as the ‘edge of chaos’ algorithm when applied to the TAP equations: we noticed that the number of iterations required to achieve convergence to a fixed point increased dramatically as the

system size  $N$  increases, or as  $\alpha$  approaches its critical value.

In the context of mean-field problems such as finding the groundstate of the SK model, the ‘edge of chaos’ algorithm works well. We have also tested it on the one-dimensional spin glass at  $T = 0$ , (which can of course be solved exactly, enabling one to easily judge the accuracy of any proposed treatment). Although it again outperformed simple descent algorithms it was hard to get solutions whose energies per spin were equal to the equilibrium energy per spin. We attribute the difference to the nature of the free-energy landscape. In one dimension the barriers around the states of the lowest energy are little different in height to those surrounding metastable states of much higher free energy.

### Acknowledgments

RAB acknowledges an EPSRC Fellowship GR/R44768 under which part of this work was conducted, and a Royal Society of Edinburgh Personal Research Fellowship under which it was completed. TA acknowledges support by the DFG under grant Zi 209/7. We thank G. Jentsch for kindly performing some of the simulations used in this work.

- 
- [1] F. Tanaka and S. F. Edwards, J. Phys. F **10**, 2769 (1980).  
 [2] A. J. Bray and M. A. Moore, J. Phys. C **13**, L469 (1980).  
 [3] D. J. Thouless, P. W. Anderson, and R. G. Palmer, Phil. Mag. **35**, 593 (1977).  
 [4] G. Parisi and T. Rizzo, J. Phys. A **37**, 7979 and references therein (2004).  
 [5] T. Aspelmeier, A. J. Bray, and M. A. Moore, Phys. Rev. Lett. **92**, 087203 (2004).  
 [6] A. Cavagna, I. Giardinà, and G. Parisi, Phys. Rev. Lett. **92**, 120603 (2004).  
 [7] T. Castellani and A. Cavagna, cond-mat/0505032 and references therein (2005).  
 [8] S. Boettcher and M. Frank, cond-mat/0509001 (2005).  
 [9] A. J. Bray, H. Sompolinsky, and C. Yu, J. Phys. C: Solid State Phys. **19**, 6389 (1986).  
 [10] M. Mézard, G. Parisi, and M. A. Virasoro, *Spin glass theory and beyond* (World Scientific, Singapore, 1987).  
 [11] T. Plefka, Phys. Rev. B **65**, 224206 (2002).  
 [12] C. G. Broyden, Math. Comput. **19**, 577 (1965).  
 [13] *The GNU scientific library (GSL), version 1.4*, URL <http://www.gnu.org/software/gsl>.  
 [14] T. S. Grigera, A. Cavagna, I. Giardinà, and G. Parisi, Phys. Rev. Lett. **88**, 055502 (2002).  
 [15] W. H. Press, B. P. Flannery, S. A. Teukolsky, and W. Vetterling, *Numerical recipes in C* (Cambridge University Press, Cambridge, 1992).  
 [16] D. H. Bailey, Y. Hida, K. Jeyabalan, X. S. Li, and B. Thompson, *Arbitrary precision package (ARPREC)* (2005), URL <http://crd.lbl.gov/~dhbailey/mpdist/index.html>.  
 [17] A. Crisanti and T. Rizzo, Phys. Rev. E **65**, 046137 (2002).  
 [18] A. Crisanti, L. Leuzzi, G. Parisi, and T. Rizzo, Phys. Rev. B **68**, 174401 (2003).  
 [19] T. Rizzo, *private communication*.  
 [20] C. M. Newman and D. L. Stein, Phys. Rev. E **60**, 5244 (1999).  
 [21] G. J. Rodgers and M. A. Moore, J. Phys. A **22**, 1085 (1989).